Keggin Polyoxoanions in Aqueous Solution: Ion Pairing and Its Effect on Dynamic Properties by Molecular Dynamics Simulations

Frédéric Leroy,[†] Pere Miró,[‡] Josep Maria Poblet,[§] Carles Bo,*[,‡,§] and Josep Bonet Ávalos*[,†]

Departament d'Enginyeria Química, ETSEQ, Universitat Rovira i Virgili, Avinguda dels Països Catalans 26, 43007 Tarragona, Spain, Institute of Chemical Research of Catalonia (ICIQ), Avinguda dels Països Catalans 16, 43007 Tarragona, Spain, and Departament de Química Física i Inorgànica, Universitat Rovira i Virgili, Avinguda Marcel.li Domingo s/n, 43007 Tarragona, Spain

Received: September 4, 2007; Revised Manuscript Received: April 30, 2008

The dynamics of Keggin polyoxoanions in aqueous solution in the presence of monovalent cations is analyzed through molecular dynamics simulations. Together with structural information yielding the radial distribution functions of Li^+, Na^+, and K^+ with three polyoxometalates (POMs) bearing 3−, 4−, and 5− charges, the diffusion coefficient of these POMs is calculated. We found that the effect of the microscopic molecular details of the solvent is a key aspect to interpreting the structural and dynamic data because a competition between electrostatic interactions between the ions and the stability of the solvation shell is established. Furthermore, we show that solvent-shared structures weakly bound to the POM anion play a crucial role in the determination of the dynamic properties of the anion. The nature of these ion pairs, structurally characterized for the first time, is consistent with experimental data available.

Introduction

Ion pairing is invoked as a ubiquitous effect that plays a relevant role in a broad range of chemical phenomena. It is well-known that the formation of long-lived pairs of ions in solution is responsible for numerous physicochemical properties like electric conductivity, redox properties, electron transfer,[1–3] and chemical reactivity[4] among others. It largely determines ion transport[5] or dynamical behavior[6] in biological systems. Recently, Marcus and Hefter[7] comprehensively reviewed the experimental methods in use nowadays to assess and characterize the existence and the effects of ion pairing, as well as theories dealing with the phenomenon. Also, the tremendous impact that ion pairing has on transition-metal organometallic chemistry and homogeneous catalysis has been reviewed.[8,9] From the theoretical point of view, the fundamentals of ion pairing were described by Bjerrum,[10] who analyzed the properties of ions bearing point charges immersed in a continuum. Besides this primitive model of electrolyte solutions,[11] atomistic simulations enabled the study of the dynamical evolution of molecular systems by considering, in explicit form, both the solute and the solvent and, in particular, the effects of the microscopic details of the ion−ion and ion−solvent potentials beyond pure electrostatic interactions. In the last years, molecular dynamics simulations have been able to quantitatively reproduce experimentally measured structural properties of ion pairs in systems of increasing complexity,[12–18] and it has been revealed as a powerful tool to characterize the different sorts of ion pairs.[19] According to the literature,[7] three distinct situations have been described: namely, contact ion pairs (CIPs), solvent-separated ion pairs (2SIPs), and solvent-shared ion pairs (SIPs). In this article, we will focus our attention on the effect of the pairing on dynamic properties of polyoxometalate (POM) anions in aqueous solution, especially with regard to the structure of the cations around a given anion.

A large class of transition-metal−oxygen anion clusters are described under the name of POMs.[20–22] Their size and shape span a broad range, from the smallest hexatungstate $[W_6O_{19}]^{2-}$ anion to the giant nanocapsules that contain 368 molybdenum atoms introduced by Müller et al.[23] POMs have found application in a variety of disciplines,[24] their redox properties have been applied to a number of catalytic processes,[25–30] some of them present extraordinary magnetic behavior,[31] they may be present in nuclear waste,[32] and these kinds of compounds have even been applied in medicine.[33] More recently, their applications in energy storage systems,[34–36] in nanodevices,[37] or as models of artificial cells[38–41] have been reported. Regarding these porous nanocapsules, the dynamic structure of encapsulated water molecules and the uptake and release of cations are topics of much interest.

Aimed at dealing with those dynamic phenomena and after studying the electronic structure and reactivity of some POMs,[42–48] we recently reported a molecular dynamics based study on the structure of solvent water molecules around Keggin anions.[49] Indeed, the Keggin anion is one of the most relevant members of the POMs' family with the general formula $[XW_{12}O_{40}]^{n-}$, where X can be a main-group element (P, Si, Al, Ge, etc.) or a transition-metal ion (Fe, Co, Cu, etc.). The so-called α-Keggin structure sketched in Figure 1 is based on a central $[XO_4]$ tetrahedron and a $[W_{12}O_{36}]$ addendum. As can be seen in Figure 1, three distinct types of oxygen atoms can be distinguished: the four XO_4 oxygen atoms (labeled O_{tetra}) are isolated from the external surface, 12 external oxygen atoms labeled O_{term} are located at the furthest distance from the central atom of the anion, and 24 oxygen atoms labeled O_{bridge} are bridging $[WO_6]$ octahedra. By using an electrochemical methodology, Pope and Varga[50] obtained the diffusion coefficients of $[PW_{12}O_{40}]^{3-}$ (PW_{12}) and $[SiW_{12}O_{40}]^{4-}$ (SiW_{12}) among other anions and found

* To whom correspondence should be addressed. E-mail: cbo@iciq.es (C.B.), josep.bonet@urv.cat (J.B.A.).
† Departament d'Enginyeria Química, ETSEQ, Universitat Rovira i Virgili.
‡ Institute of Chemical Research of Catalonia.
§ Departament de Química Física i Inorgànica, Universitat Rovira i Virgili.

10.1021/jp077098p CCC: $40.75 © 2008 American Chemical Society
Published on Web 07/01/2008

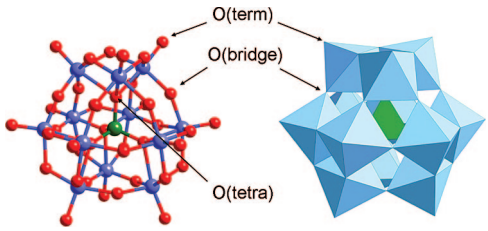

Figure 1. α-Keggin $[XW_{12}O_{40}]^{n-}$ anion.

a value of 5.6 Å for their hydrodynamic radius. More recently, an experimental study of ion pairing in solutions containing POMs has been reported by Grigoriev et al.[51,52] Indeed, Grigoriev et al. carried out electrochemical measurements to obtain the diffusion coefficient of a series of $[XVW_{11}O_{40}]^{z-}$ vanadium-substituted Keggin anions with different monovalent cations in water−*tert*-butyl alcohol (TBA) solutions. When viscosity measurements of the solutions were performed and the Stokes−Einstein law was used, a hydrodynamic radius R_H was assigned to the anion in its particular environment. These authors reported that R_H was invariant under the exchange of the different cations in pure water solutions, as was found by Pope et al. This was interpreted as the anions remain bare most of the time; that is to say, no ion pairs are significantly formed in the system. On the contrary, the radius was observed to vary when given mixtures of TBA and water were used. It was then concluded that ion pairing was effective in the water−alcohol mixture while it was not in pure water. This behavior is mostly due to the fact that the dielectric constant of water and that of the mixture of water and alcohol used by Grigoriev et al. differ by a factor of more than 2.[53] The formation of ion pairs was favored as a consequence. Moreover, $[AlW_{12}O_{40}]^{5-}$ (AlW_{12}) recently received attention as a well-behaved model for investigating an outer-sphere electron-transfer process in water.[54] Furthermore, it has been shown that monovalent cations catalyze anion−anion electron-transfer reactions,[55] and although it was assumed that ion pairs do not form in those conditions, the catalytic effect was explained by the presence of partially dehydrated cations.

In this article, the long-time dynamics of some α-Keggin anions in water is classically analyzed. In particular, three Keggin anions, namely, PW_{12}, SiW_{12}, and AlW_{12}, have been considered in different water solutions made neutral with Li^+, Na^+, and K^+ cations. We focus our attention on the analysis of the ion pairing and its dependence in the Keggin anion charge as well as the kind of monovalent cation present in the system. Mention should be made of the fact that our interpretation of pairing relies on energetic considerations based on Bjerrum's original picture. Our approach is justified by the relation between the potential of mean force and the time of life of the association. Because our goal is only to rationalize the observed dynamics by referring it to the common concept of ion pairing, the question of whether a different definition is more appropriate is immaterial for our purpose. Nevertheless, in a wider context of the theoretical analysis of the thermodynamic properties of electrolyte solutions, the subtleties of the definition may be important.[56]

On the one hand, we provide here a description of the structure of these pairs, which is lacking for these kinds of anions. The complexity of the structures arises from the effect of the solvent on the interactions between the ions. It was recently shown that this effect is of crucial importance in the analysis of some electrostatic phenomena.[57] It was also remarked that the molecular nature of the solvent influences the description of the interaction of ions in solution.[58] On the other hand, we study the effect of ion pairing on measurable dynamical properties, as the POM diffusion coefficient. Our analysis reveals a complex interplay between the solvation shell of the cation and the direct anion−cation electrostatic interactions. This interplay permits us to infer the cause of the nonmonotonic behavior of the diffusive properties of the anions with respect to both the anion charge and the cation size.

The structure of the paper is as follows: in the second section, we will briefly discuss the theoretical considerations required for the analysis of the simulation results. We address the reader to the Supporting Information for a complete description of the computational details. Subsequently, we devote the third section to a detailed analysis of the simulation results, both static and dynamic. Finally, in the last section, we address the conclusions drawn from this study.

Background and Computational Details

Theoretical Background. The concept of ion pairing was first introduced by Bjerrum[10] at the beginning of the last century. Bjerrum considered a system of spherical hard ions with a definite size embedded in a continuous dielectric solvent characterized by its permittivity and submitted to thermal fluctuations. When analyzing the behavior of this system around a test ion, he found that, if this central ion and the counterion cloud have opposite charge, counterions will have a tendency to gather at a short distance from the central ion determined by excluded-volume interactions. Moreover, at the regions where the electrostatic energy is less than the thermal energy k_BT, the counterions will be dispersed by thermal fluctuations, while at the regions where the electrostatic energy is higher than the thermal energy, the counterions will be strongly bound to the central ion.

More in detail, Bjerrum determined the probability of finding a counterion at a given distance from the test ion using the model described above, where the interactions between the different ions are only hard-core repulsions and electrostatic, with the solvent being considered as a structureless medium with a given electric permittivity. He found that this probability has a minimum at a characteristic distance λ_B given by

$$\lambda_B = \frac{|z_+ z_-| e^2}{2\epsilon k_B T} \tag{1}$$

since then referred to as Bjerrum's length. It is interesting to remark that, under certain conditions of solvent quality given by ϵ and valence of the ions, Bjerrum's length can extend to the nanometer scale. Furthermore, it must be noticed that the ratio between electrostatic and thermal energy is a factor of 2 when the distance between the counterions is λ_B. Therefore, from a physicochemical point of view, it is customarily considered that counterions whose distance to the central ion is less than λ_B are paired with the central ion. This definition is, however, arbitrary because counterions having an energy in between k_BT and $2k_BT$ can still form relatively long-lived associations despite the fact that they would not be considered as paired under this criterion. Much has been written with respect to the definition of ion pairs, and different points of view and recipes have been adopted in the framework of a thermodynamic theory of electrolytes considering ionic pairs as chemical species.[56,59] Among others, the problems underlying this chemical perspective are (a) the proper account of all contributions to the free energy[60] as well as (b) the issue of using association constants in all temperature ranges.[61] Nevertheless, the micro-

scopic analysis that we address in this article is affected by none of these problems because, on the one hand, the definition of an ion pair depends essentially on the criterion chosen (more or less convenient) to discriminate associated and dissociated pairs.[60,56] On the other hand, the temperature of our treatment is low enough so that we prevent negative values of the dissociation constant from occurring because of a decrease of Bjerrum's length below the hard-core radius of the ions.[61] Thus, in our interest of rationalizing the dynamic behavior of POM anions in solution in terms of the existence of anion−cation associations, we have adopted the simple original Bjerrum criterion to discriminate long-lived pairs from looser associations.

The problem that we aim at treating in this study involves effects due to the finite size and polarity of the solvent, as well as the complex charge distribution beared by the anions. In this framework and in view of the energetic perspective that we have just mentioned, Bjerrum's length cannot simply be obtained from eq 1. To obtain a measure of Bjerrum's length, and therefore the criterion through which we identify a long-lived pair, let us consider that the average number density of cations at a distance r from the center of a tagged anion in a spherically symmetric problem can be expressed as[62]

$$n_+(r) = n_+^0 g(r) \tag{2}$$

where $g(r)$ is the pair distribution function between the anion and the corresponding cation, often referred to as the radial distribution function (RDF) due to its spherical symmetry, and n_+^0 is the bulk cation number density. In general, we can express $g(r)$ as[7]

$$g(r) \equiv \mathrm{e}^{-W(r)/k_\mathrm{B}T} \tag{3}$$

This expression defines $W(r)$ as being a free energy of the system anion−cation at a distance r. $W(r)$ is referred to as the potential of mean force between the ions.[69] The potential of mean force contains all of the electrochemical effects, involving excluded-volume interactions, polarizability, and the molecular structure of the solvent as well as electrostatic interactions between the ions in the system. Therefore, when $-W(r)/k_\mathrm{B}T > 2$, we can consider that ion pairs can exist because the free energy is negative and larger in absolute value than twice the thermal energy. Thus, from the measure of the pair distribution function, we can state that for our system Bjerrum's length is given by the relation

$$-\frac{W(\lambda_\mathrm{B})}{k_\mathrm{B}T} = \ln g(\lambda_\mathrm{B}) = 2 \tag{4}$$

Finally, the number of pairs N_+ would be obtained by using

$$N_+ = 4\pi n_+^0 \int_0^{\lambda_\mathrm{B}} r^2 g(r)\, \mathrm{d}r \tag{5}$$

A similar perspective for introducing the nonelectrostatic effects due to the structure of the solvent can be found in the literature.[7,58,63] Despite the fact that the theoretical approach outlined so far permits one to describe systems within regions where $-W > 2k_\mathrm{B}T$, the properties of electrolyte solutions also depend on regions where $k_\mathrm{B}T < W < 2k_\mathrm{B}T$. In that case, the anion−cation structure still exists for a significant time. We show in what follows that the configurations characterized by $k_\mathrm{B}T < W < 2k_\mathrm{B}T$ have an important impact on the diffusive behavior of POMs.

Computational Details. In the present approach, we study the long-time collective behavior. We used a large number of solvent molecules to describe high dilution conditions for the POMs, as close as possible. The methodology employed is molecular dynamics simulations, which describe trajectories of the system in phase space. No explicit reference to the electronic structure is made beyond the ultimate electronic origin of the effective interaction potentials used.

Molecular dynamics simulations were carried out using the DLPOLY package.[64] We address the reader to the Supporting Information for a complete description of the parameters and procedures, as well as for definitions of the molecular models used. All of the systems analyzed contain 1000 water molecules, 1 anion, and a number of cations ranging from 3 to 5, depending on the net electrostatic charge of the anion, so that the system is neutral overall. This represents an anion concentration of about 5.4×10^{-2} mol/L. We have also carried out simulations on test systems containing 8000 water molecules, 8 anions, and the corresponding number of cations, at the same concentration, to check that our results are independent of the size of the system when its size is increased by roughly 1 order of magnitude. Hence, the results of our analysis physically correspond to those of a system with the mentioned POM concentration, and no finite-size effects are present. Simulations to determine the behavior of the system at infinite dilution of POM lie beyond the scope of the present work. The total length of independent simulation runs ranges from 5 to 7 ns, which permitted us to obtain statistically reliable results even with that small number of ions present in the system. The parameter set used for water molecules corresponds to that of the SPC/E model.[65] The monovalent cations used are Li^+, Na^+, and K^+, whose models are described in the work of Lee and Rasaiah.[66] The set of Lennard-Jones parameters and charges of the anions was taken from our previous work[49] or generated in an equivalent manner.

The analysis of the structures of the POMs in solution has been done through the calculation of anion−cation RDF $g(r)$, which is proportional to the probability of the presence of a cation at a distance r from the center of the POM anion. The calculations are angle-averaged, i.e., insensitive to the distribution of the oxygen atoms at the surface of the POMs, but still contain enough information about the structure of the cation corona around the Keggin anion. One of the major technical difficulties of our analysis is the lack of data required for the evaluation of the RDF per trajectory due to the reduced number of ions in the system. As a consequence, long simulation runs are required to produce statistically significant data. Besides the direct simulation of the system, other methods have been devised to deal with the statistics of ionic systems consisting of few significant particles and long-lived events that may impair a correct sampling of phase space.[58] We checked in the present study that the lifetime of the ion pairs is short enough compared to the total length of the simulation. Much formation and breaking of pairs was observed during the simulation. Therefore, this phenomenon is correctly sampled.

With the purpose of evaluating the impact of the ion-pair formation on the dynamic properties of the POM molecule, we computed the self-diffusion coefficients of the anions PW_{12}, SiW_{12}, and AlW_{12} as a function of the cations Li^+, Na^+, and K^+, through the Einstein relation

$$D = \frac{1}{6} \lim_{t\to\infty} \frac{\mathrm{d}}{\mathrm{d}t} \langle |r(t) - r(0)|^2 \rangle \tag{6}$$

where $\langle \cdots \rangle$ refers to an equilibrium average, which in *NVT* simulations corresponds to that of the canonical ensemble. It should be noticed that the asymptotic diffusive behavior of the mean-square displacement of the POM with respect to time is reached quite fast (a few picoseconds) for such a colloid-like particle dissolved in a solvent of much smaller particles at liquid

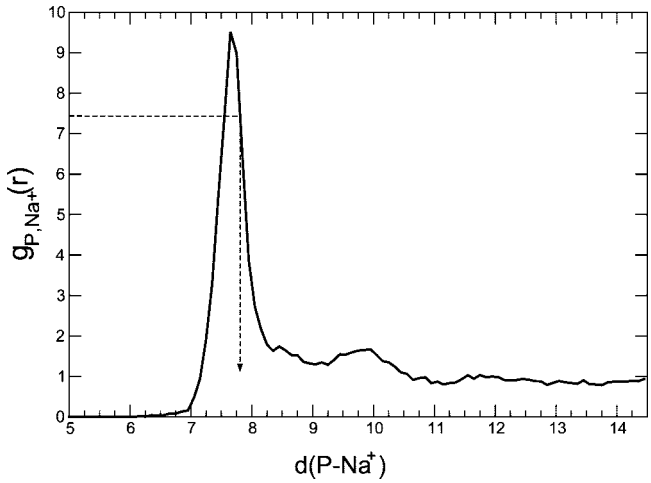

Figure 2. RDF of the pair P−Na^+ in the (PW_{12}, three Na^+ cations) system. Distances are in Angstroms. The dotted arrow shows the solution of eq 4 and, hence, the location of Bjerrum's length.

density. Then, from the computational point of view, this fact and the time translational invariance of the dynamic properties of the system in thermodynamic equilibrium permits us to use several time windows, sufficiently decorrelated, of a single trajectory run of the POM in solution to evaluate the average of eq 6, with reasonably good statistics. The diffusion coefficient of the anion in each system has been then obtained from the calculation of its mean-square displacement during the run.

Results and Discussion

Structure of the Ionic Systems. The calculated trajectories of the system during the simulations provide the distribution of ions around the Keggin anion through the evaluation of pair RDFs. In this section, we consider these pair distribution functions for three different anions (either with a phosphorus, silicon, or aluminum as the central atom of the Keggin) with three different cations (lithium, sodium, or potassium). A typical shape of these RDF functions is shown in Figure 2, corresponding to PW_{12} anion with three Na^+ cations.

The figure exhibits well-defined features. A first maximum is located at a distance of 7.7 Å from the center of the anion. A second one, broader than the first, is centered around 9.9 Å and is separated by a shoulder structure. In what follows, we will give a physical interpretation of these structures. First of all, because the distance between the central phosphorus atom of the anion and a terminal oxygen (O_{term}) is 5.29 Å (cf. Table 3 in the Supporting Information) and taking into account that the Lennard-Jones soft-sphere diameter of a O_{term} and that of a sodium cation are respectively 3.17 and 2.58 Å (cf. Tables 3 and 2, respectively, in the Supporting Information), the first maximum can clearly be identified as the signature of a long-lived close contact between the anion and one of the cations. More precisely, this contact occurs through one of the O_{term} atoms of the Keggin anion. The peak is located at a shorter distance than the sum of the Lennard-Jones radii of the particles, 5.29 + 3.17/2 + 2.58/2 = 8.16 Å, because of the fact that the O_{term} protrudes into the solution, leaving space for the cation to move around the O_{term}. In this way, the cation is closer to the center of the anion during these *excursions*. In addition, such a behavior has been observed by direct inspection of the simulated trajectories. We show in Figure 3 a snapshot of such a direct contact between a $[PW_{12}O_{40}]^{3-}$ anion and one of the three sodium cations.

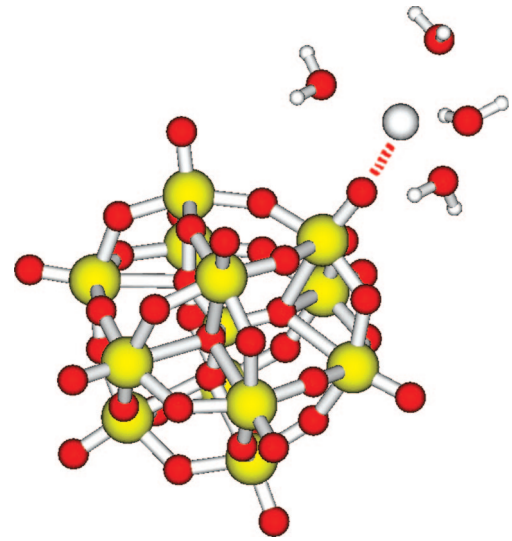

Figure 3. Illustration of a direct contact between a sodium cation and one O_{term} of the PW_{12} anion. The represented water molecules have their oxygen atom at a distance shorter than 3.5 Å from the cation. The dashed red line is represented as a guide for the eye.

TABLE 1: Bjerrum's Length of the Set of Studied Systems Computed by Using (4) and the Number of Formed Pairs As Computed by Using the Definition (5)

	λ_B /Å			N_+		
	Li^+	Na^+	K^+	Li^+	Na^+	K^+
$[PW_{12}O_{40}]^{3-}$		7.8			0.24	
$[SiW_{12}O_{40}]^{4-}$		7.9	8.2		0.85	0.35
$[AlW_{12}O_{40}]^{5-}$	7.4	7.9	8.2	1.72	1.00	0.78

Following the procedure described above, Bjerrum's length is obtained by solving eq 4 for each system using the numerically calculated RDFs. The values obtained by this methodology, as well as the averaged number of paired cations computed using the definition (5), are reported in Table 1.

Then, considering Bjerrum's length of the system (PW_{12}, three Na^+) and Figure 2, we concluded that the structure corresponding to the first peak can be referred as a contact ion pair (CIP),[7,9] because of the fact that the peak is located at a distance shorter than Bjerrum's length and, therefore, its potential of mean force is larger than $2k_BT$. When the SiW_{12} and AlW_{12} anions are considered, with the same Na^+ cation that we notice from Table 1, Bjerrum's length remains almost constant under the exchange of the anion. This can be interpreted also as a signature of the CIP because the effect of the increase in the anion charge is compensated for by the repulsive part of the potentials (close to a hard-core repulsion), where the anions have almost the same size. On the other hand, the number of pairs formed with the anion, N^+, is ordered following P < Si < Al, i.e., following the sequence of an increase of the anion charge. This is clearly related with the enhancement of the CIP peak on the RDF plot of Figure 4. The values obtained for N_+ below 1 reveal that the ion pairs formed are not permanent and a significant exchange between cations occurs. This dynamical behavior of a CIP is illustrated in Figure 5, where the distance between each sodium cation and the center of the POM is shown as a function of time. Note the different events of close proximity giving rise to long-lived cation−anion contacts on the order of hundreds of picoseconds, which statistically we define as CIP. Indeed, the relative duration of these close contact events with respect to the total simulated time is approximately the calculated average number of cations paired, N_+.

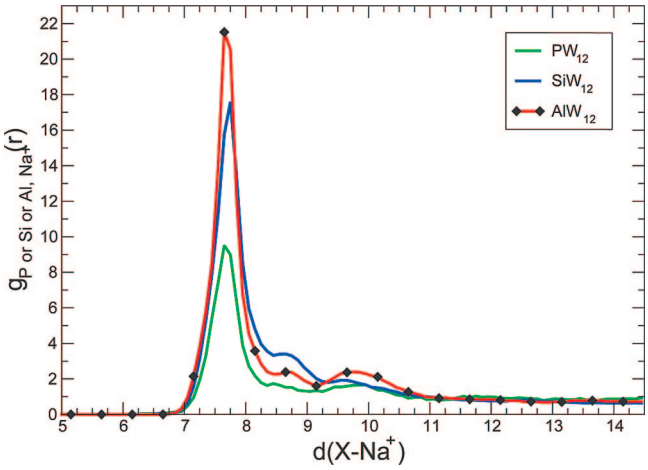

Figure 4. RDF of the pair X−Na^+ in the PW_{12}, SiW_{12}, and AlW_{12} systems. The estimation of the error in the RDF ranges from 0.3% for the CIP peak to 13% at around 14 Å, where no structure is observed. Distances are in Angstroms.

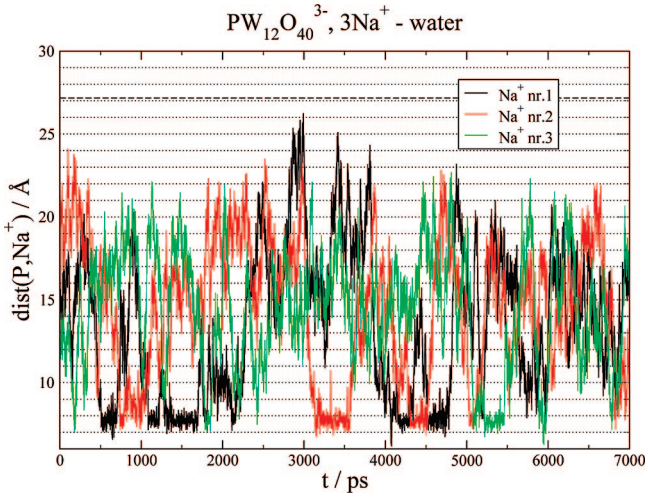

Figure 5. Evolution of P−Na distances for the system (PW_{12}, three Na^+) during a 7 ns simulation. Every line corresponds to a different cation.

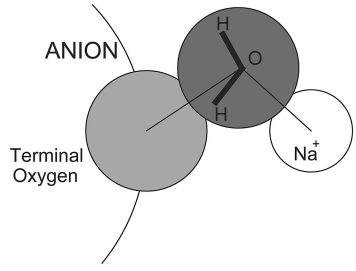

Figure 6. Simplified two-dimensional illustration of a solvent-shared ion pairing between the PW_{12} anion and Na^+. The mean value of the angle O_{term}−O_{water}−Na^+ is 127°. The mean value of the distance between O_{term} and Na^+ is 4.75 Å. The mean value of the angle between O_{water} and O_{term} and the dipolar moment of the water is 43°.

The second maximum around 9.9 Å appearing in Figures 2 and 4 is outside of Bjerrum's sphere and, therefore, cannot be accounted for an ion pair because the binding free energy of the arrangements is lower than $2k_BT$. Nevertheless, this structure, illustrated in Figure 6, corresponds to a solvent-shared configuration of the system. It should also be remarked that in this last structure some water molecules have a tendency to be simultaneously in contact with both the O_{term} of the anion and cation, bridging them. Typical plots of the RDF of water around

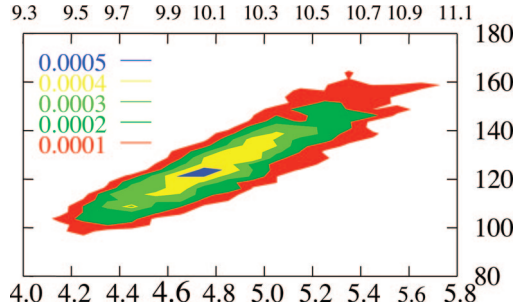

Figure 7. Angle (O_{term}−O_{water}−Na^+) as a function of the distance O_{term}−Na^+ (lower scale) or P−Na^+ (upper scale) in (PW_{12}, three Na^+) system. The color represents the probability of obtaining the correlation between the distance and the angle.

the anions have been reported in our previous work[49] and the structure of water around the cations has been analyzed by Lee and Rasaiah.[66] To determine the role of the solvent in stabilizing the cation in that particular position, we plotted a histogram of the events where the cation is at a given distance of the terminal oxygen and, simultaneously, the angle formed by the species cation−O_{water}−O_{term} has a given value. Among all water molecules, only the closest ones have been retained. In this way, we can see the correlation between the position of the second maximum in the RDF and the conformation of the surrounding water molecules.

The histogram of these events is shown in Figure 7. The extension of the contour depends on the variations of the parameters; nevertheless, we are particularly interested here in the shape of the curve and the location of the maximum. A maximum can clearly be identified, indicating a correlation between the relative anion−cation position and the angle formed with the surrounding water molecules. We found an average distance of 4.75 Å and an angle of around 127°. The distance is in line with a distance cation−O_{term} of about 5 Å based on the atoms' hard-core radii given by half of the Lennard-Jones diameters. The fact that the angle cation−O_{water}−O_{term} is larger than 109.47° (corresponding to the angle between two vertices in a tetrahedron) indicates that the water molecules placed between the cation and O_{term} are tangent to each other. Moreover, the width of the distribution suggests a kind of breathing movement during which water sidesteps when the cation approaches the terminal oxygen. The distances then appear slightly shorter because of the pendular motion of the whole structure around the terminal oxygen, which on average makes it be closer to the anion center. Therefore, the analysis of this solvent-shared structure suggests that it is formed by the contact between the terminal oxygen and the water molecules, forming the cation first solvation shell. Furthermore, this structure is stabilized by the existence of hydrogen bonds between the terminal oxygen of the anion and these water molecules in the solvation shell of the cation, without an appreciable distortion of this latter structure.[49] Shorter or larger distances between the Keggin anion and the cation are thus not favored by the stability of the water solvation shell, except when this water shell is completely opened and a CIP arises. The events giving rise to this secondary peak can also be seen in Figure 5. Note the portions of the cation trajectories where the particle lies around 10 Å from the center of the anion. We want to point out that the importance of the molecular size of the water molecules acting as a solvent placed between charged entities was also recently addressed in another context.[57]

Beyond the CIP structure, a shoulder exists between the tight contact state and the cation solvated structure identified above

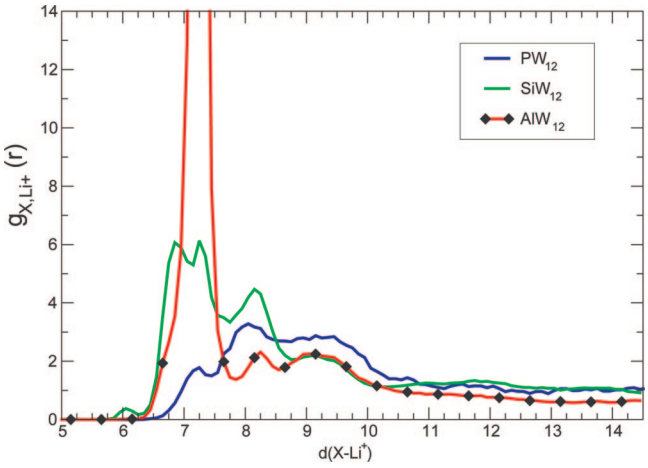

Figure 8. RDF of the pair X−Li^+ in the PW_{12}, SiW_{12}, and AlW_{12} systems. Distances are in Angstroms.

9.9 Å. The height of this shoulder does not follow the anion-charge ordering. The presence of this structure may suggest that the preferred positions for the anion and cation are either the CIP or a loose pair formed by the anion and a solvated cation, fluctuating between structures that are less convenient accommodations of the solvent molecules but still energetically favorable.

Finally, the (PW_{12}, three Na^+), (SiW_{12}, four Na^+), and (AlW_{12}, five Na^+) systems do not show any structure beyond 12−13 Å from the center of the anion, with the RDF being in addition approximately 1 in this region. Hence, the only ion-pairing states that we can describe here are CIP, despite the presence of SIP-like structures outside Bjerrum's sphere.

When the potassium cation is considered instead of sodium in a neutral solution with each of the anions mentioned above, a close analogy with the corresponding previously discussed system is observed, and thus the qualitative behavior is the same. We then address the interested reader to the Supporting Information for the details of the RDF behavior of the systems PW_{12}, SiW_{12}, and AlW_{12} in the presence of the corresponding number of K^+ cations.

A significantly different scenario occurs when lithium cations are present. As can be seen in Figure 8, several maxima exist in the RDF of the different anions. Three structures can then be suggested at different locations for the three anions. The first one corresponds to the same CIP maximum observed for the Na^+ cations. However, according to Table 1, Bjerrum's length for P and Si POMs is not defined for these systems with Li^+ cations and only the AlW_{12} POM unequivocally presents a stable CIP. For the other anions, the structure corresponding to this CIP is energetically less favorable. The second maximum around 9 Å identified as a solvent-shared structure in the previous cases is also present for the Li^+ cations. Moreover, with respect to the previously analyzed cases where only two maxima were present, an intermediate maximum appears here at around 8.25 Å at the location where only a shoulder, or simply a region between maxima, was observed before. The structure represented by the intermediate maximum suggests also a solvent-shared state.

In the case of PW_{12} anion, the clear structure of two maxima, corresponding to a very frequent CIP structure together with a less populated solvent-shared configuration as observed for Na^+ and K^+ cations, has disappeared. In the case of Li^+, it is replaced by a broader overall structure with three maxima. We can argue that the first peak located around 7.25 Å is reminiscent of the CIP structure. However, the Li^+ cations in this position do not fulfill Bjerrum's criterion to define a strongly bound state. The second maximum at 8.2 Å and the third at around 9.1 Å can both be considered as solvent-shared structures corresponding to different arrangements of the water molecules bridging the cation with the POM. Although our analysis does not yield a clear explanation, we think that the solvent-shared structure is formed by water molecules bridging the terminal oxygen and the cation, causing only a slight distortion of the cation solvation shell. It has been reported that, with the model used here,[66] the small size of the Li^+ cation makes the solvation shell be more stable than that for larger cations. Thus, the stability of this solvation shell around the cation competes with the electrostatic attraction of the relatively weakly charged PW_{12} anion, leading to the observed population distribution of the cations among the different structures in Figure 8.

In the case of the SiW_{12} anion, the increase of the electrostatic charge of the anion changes the previous picture by enhancing the intensity of the first peak, without forming a stable CIP assembly, probably because of the distortion of the Li^+ solvation shell. The detailed structure of the RDF is, however, complex. We clearly observe the presence of the intermediate solvent-shared structure peak at 8.2 Å, which is more intense than that in the case of PW_{12}. However, the solvent-shared structure at around 9.1 Å, beyond Bjerrum's length, is less intense for the silicon anion than for the phosphorus one. Finally, when AlW_{12} is considered, a dramatic change in the structure is observed. Effectively, the CIP assembly is almost the only significant state observed from the RDF. Indeed, the CIP maximum has an intensity about 10 times larger than that of the other anions. When the distance Al−Li is plotted with respect to time, it is seen that one of the cations remains in close contact with the anion during the whole 7-ns simulation run. This indicates that the Li^+ cation is so strongly bound to the AlW_{12} anion that the escape time is on the order of or larger than the overall simulation time. Moreover, the two other cations behave similarly during several hundreds of picoseconds and even during a few nanoseconds, yielding the high averaged number of pairs reported in Table 1. This implies that the secondary structures that the system can form are rarely encountered as compared with the CIP one.

In this latter case, however, the analysis can only be qualitative. The fact that the lifetime of the CIP conformation is as large as the simulation itself implies that the sampling of the phase space is not properly done by this direct method, yielding, for example, a RDF that does not tend to 1 at distances of around 14 Å where the system should shows bulk features.

In summary, the analysis of the RDF reveals a rich variety of scenarios of the ion-pair associations and other long-lived structures formed between POMs and cations of different sizes. The effect of the solvent significantly distorts the intuitive picture according to which the ion-pair associations should be stronger for larger anion charge in combination with smaller cations. We can argue that for some systems the competition between the solvation effects and the electrostatic interactions between the electrolytes plays a significant role in the interpretation of the RDF data. Therefore, the picture of ion pairing occurring in a system of point charges in a continuum fails to explain the fine details of the systems studied here, essentially because of the influence of the molecular details of the solvent molecules, whose size is comparable to the cation size. Furthermore, consideration of the solvent as a continuum together with point charges swaps the complex effect of correlations between

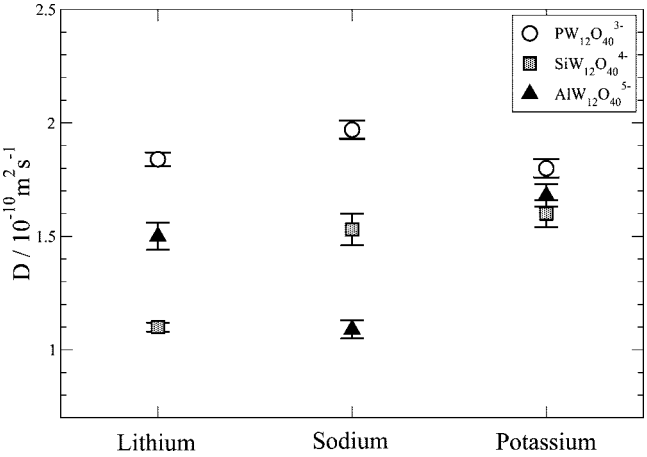

Figure 9. Self-diffusion coefficients of the Keggin anions.

solvent and electrolyte particles that are necessary to analyze the features of the RDF functions described here.

Dynamical Aspects. The association between the anion and the cations has implications also in dynamic properties like the POM diffusion coefficient, which can be measured electrochemically[51,52] or by diffusive NMR.[67] For instance, experimental data on POMs[51,52] indicate that the diffusion coefficient of the polyoxoanion varies with the quality of the solvent. We report in Figure 9 the diffusion coefficients of PW_{12}, SiW_{12}, and AlW_{12} anions for the three different cations, ordered according to their size. The statistical error is about 6%.

The obtained values for the diffusion coefficients reproduce reasonably well the order of magnitude of the experimental data for similar systems under slightly different conditions.[51,52] Indeed, diffusion coefficients for vanadium-substituted Keggin anions in a mixture of water/TBA at 60 °C range from 1.6 to 2.8×10^{-10} m^2 s^{-1}. Figure 9 indicates that the behavior of the diffusion coefficient does not follow a simple pattern, neither with the cation size nor with the anion charge. To analyze this fact, let us first center our attention on the variation of the diffusion coefficient of the PW_{12} anion with respect to the different cations considered in this work. We see that D is not a monotonic function of the cation size, exhibiting a maximum for the intermediate-size Na^+ cation. The other extreme is given by the AlW_{12} anion. In this case, the behavior is opposite to that of the phosphorus anion in the sense that, for the aluminum-containing anion, D has a minimum when the solution contains the intermediate-size Na^+ cation.

The complexity of this behavior can only be understood as a result of the competition between at least two different effects: the direct electrostatic interaction between the anion and the cation, on the one hand, and the stability of the solvation shell around the counterion, on the other hand. Hence, we can argue here that the less charged PW_{12} is unable to break the solvation shell for the smaller cation Li^+, which exhibits a tighter interaction with the water molecules because of a larger electrostatic interaction at contact, as a consequence of its smaller size. If we consider that the water forming these solvation shells, especially in the most hindered region, i.e., between the anion and the cation, cannot freely drain during the motion of the anion together with the cloud of counterions, then the friction coefficient has to be substantially larger than that one could infer from the bare counterion size. As a consequence, we state that the cations that are on average more distant from the anion center are those that will induce a larger hydrodynamic friction. Following our view based on the volume dragged along the anion and the cation, we arrived at one of the main statements drawn from this work, i.e., the idea that the diffusive properties of the paired systems do not depend on the ion-pair properties alone, as we have considered them through the energetic criterion. To rationalize our hypothesis in a more quantitative way, let us introduce a *structural* measure R_H^s of the hydrodynamic radius, which we will obtain from the static information contained in the set of $g(r)$. The *true* measure of the hydrodynamic radius, R_H, is obtained from the diffusion coefficient, making use of the Stokes−Einstein relation

$$D = \frac{k_B T}{6\pi\eta R_H} \tag{7}$$

This expression states that D should be a linear function of $1/R_H$. Thus, the proof is based on the fact that if we plot D as a function of $1/R_H^s$ and the graph yields a linear relationship between these two quantities, then we can infer that the proposed structural measure is indeed proportional to the true hydrodynamic radius as measured from the simulations, according to eq 7. The qualitative structural measure of the hydrodynamic radius that we introduce here is based on the mentioned hypothesis that the water molecules lying in the region between the cation and the anion are electrostatically hindered and contribute to the friction. We will further assume that the cation size has a subdominant effect for the problem at hand. Under these simplifying hypotheses, the only two relevant lengths in the system are the radius of the POM anion R_{anion} and the distance between the center of the cation and the surface of the POM $r-R_{anion}$. A precise hydrodynamic calculation is impossible because of the molecular nature of the problem. Thus, to estimate the extra drag induced by the presence of hindered water, we will further assume that hydrodynamically this drag is analogous to that caused by a spherical object of radius $r-R_{anion}$. This sphere would roughly be attributed to the counterion together with its solvation shell. This sphere is in contact with the anion, with the latter represented as a sphere of radius R_{anion}. These two spheres at contact would move with the same velocity, experience Stokes friction, and hydrodynamically interact with each other according to the Oseen tensor.[68] We have further averaged over all possible orientations of this tangent pair of spheres. We want to emphasize that the hypotheses made introduce a rough approximation for the hydrodynamic problem but suffice to introduce the essential ingredients as the friction and the nonadditivity of the hydrodynamic forces due to hydrodynamic interactions. A more detailed calculation would require an analysis beyond the scope of this work. By solution of the simplified hydrodynamic problem just described, the effective friction coefficient is obtained from the relation between the velocity and the total force on the ensemble. Under the hypothesis sketched above, we obtain in the limit $R/r \to 1$

$$\frac{1}{R_H^s} \simeq \frac{1}{r}[1 + (1 - R_{anion}/r) + (1 - R_{anion}/r)^2 + ...] \tag{8}$$

The value of R_H^s is obtained by extracting the value of r from the trajectory. If more than one cation is within Debye's volume, characterized by a region where the potential of mean force is on the order of k_BT, the anion contribution is considered one time, but the effect of the cations is additive. Finally, if the cation is outside the excess region, the radius is simply computed as that of the anion. In Figure 10, we have plotted the diffusion coefficient as a function of the inverse of this structural hydrodynamic radius $1/R_H^s$ averaged over the whole trajectory for each system. As can readily be seen, the data concerning the nine cation−anion systems reasonably align, thus suggesting

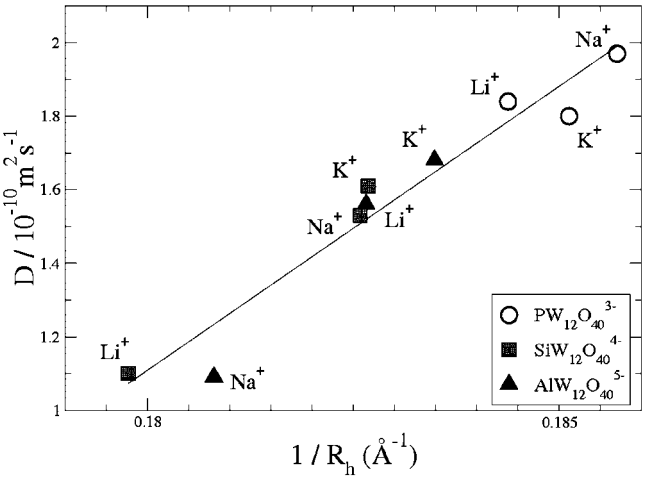

Figure 10. Self-diffusion coefficients of the anions as a function of the inverse of the structural hydrodynamic radii.

that indeed the loose structures that we have characterized as SIP are very important, as far as the dynamic properties are concerned and that the decrease of the diffusion coefficient does not necessarily imply the formation of an ion pair in the sense of Bjerrum's theory. We think that this is a remarkable result of our study. Our analysis strongly suggests that in the determination of the POM dynamic properties the existence of solvent-shared structures, which are not strictly defined as ion pairs on the basis of Bjerrum's criterion, plays a crucial role. Indeed, this structural hydrodynamic radius has been constructed, taking into account the discrete molecular structure of the solvent molecules and the cations, beyond purely continuum hydrodynamic considerations. Moreover, these solvent-shared structures have a free energy, in the sense of eq 3, larger than k_BT and, therefore, they present a long enough lifetime as to affect the diffusive dynamics of the POMs. Then, we can conclude that a lower diffusion coefficient does not necessarily imply a larger number of ion pairs, as is the case for the systems Al/Li and Al/Si.

Conclusions

In this work we have analyzed the behavior of solutions of three different POMs, $[PW_{12}O_{40}]^{3-}$, $[SiW_{12}O_{40}]^{4-}$, and $[AlW_{12}O_{40}]^{5-}$, with respect to three different monovalent cations Li^+, Na^+, and K^+. The analysis has been done by characterizing the structures by means of an energetic criterion based on the relative value of the mean-force potential of the counterion as compared with the thermal energy k_BT. This idea is reminiscent of Bjerrum's theory. In addition, we used qualitative concepts of CIP and SIP. The main conclusions drawn from our study are as follows:

(a) From a static point of view, the analysis of the RDF allowed us to identify Bjerrum's length λ_B based on the mentioned energetic criterion and calculate the number of ion pairs formed for each cation−anion system. The number of formed pairs increases with an increase in the anion charge.

(b) The detailed analysis of the different RDF indicates a quite complex behavior that cannot be anticipated by simply invoking the electrostatic interaction between the cation and the anion in a dielectric continuum. For the least-charged anion $[PW_{12}O_{40}]^{3-}$, the larger size cations Na^+ and K^+ form paired structures that we have identified as CIP.

(c) The behavior of the smaller Li^+ cation is completely different, with the blurred solvent-mediated structures SIP being more frequently encountered than the CIP ones. For the most-charged anion $[AlW_{12}O_{40}]^{5-}$, these SIP structures evolve to a strongly bound CIP structure. Nevertheless, our results can only be qualitative for this latter case because of the long lifetime of the CIP structure, on the order of the simulation time.

(d) The dependence of the diffusion coefficient on the charge of the anion as well as on the size of the cation is not simple. It depends in each case on the dominant effect, namely, either the direct electrostatic interaction at contact or the stability of the solvation shell.

(e) The representation of the diffusion coefficient with respect to the inverse of the structural hydrodynamic radius shows a proportionality that supports consistency between structural and dynamic data. Thus, our analysis supports the idea that the loose distant structures, characterized by a free energy on the order of k_BT, weaker than the tight CIP ion pairs, play an important role in the diffusion coefficients of objects like the Keggin anion.

(f) The diffusive behavior found in our analysis is slightly different from that experimentally observed by Grigoriev et al.[51,52] for vanadium-substituted Keggin anions at lower concentrations and in a different solvent. These authors reported the variations of the diffusion coefficient as being monotonic with respect to the cation size. We believe that at a low concentration ratio the stability of the cation solvation shell is not disturbed by electrostatic interactions with the anion. Thus, monotonic features are expected. Grigoriev et al. have also mentioned that the paired state conjectured from their experiments was identified as a SIP one. Moreover, these authors noticed that the smallest, more intimate, pair was formed with K^+, while the largest was formed with Li^+. Then, the solvent volume dragged should be larger for Li^+ than for K^+, leading to a faster diffusive behavior of the anions associated with K^+, as remarked by Grigoriev et al. This is in complete agreement with the arguments that we have developed in this article. Considering that the anions, the solvent, the dilution ratio, as well as the temperature used in both studies are different, we can consider that the results are rather consistent.

In summary, we have studied the subtle interplay between electrostatic interactions and the proximity effects due to the molecular structure of the solvent. The image of the ion pair as a well-defined molecular conformation has to be substituted by a more dynamic picture in which the paired ions move inside the region bounded by Bjerrum's length, with some preferred locations that are the result of the more stable balance between electrostatic interactions, entropic effects, as well as interactions mediated by the solvent.

Acknowledgment. F.L. thank the Spanish Ministerio de Educación y Ciencia (MEC) for a postdoctoral fellowship. P.M. is thankful to the Generalitat de Catalunya for a FI fellowship (2007FIC00043) supported by University and Research Commission of Innovation, University and Enterprise Department of Catalan Government, and European Social Fund. We are indebted to the MEC of the Government of Spain (Grants CTQ2005-0609-C02-02/BQU, CTQ2004-03346/PPQ, and CSD2006-0003), to the CIRIT of the Catalan Government (Grants SGR01-00315, 2005SGR00715, and 2005SGR00104), and to the ICIQ Foundation for financial support. DL_POLY is a molecular dynamics simulation package written by W. Smith, T. R. Forester, and I. T. Todorov and has been obtained from CCLRC Daresbury Laboratory via the website http://www.ccp5.ac.uk/DL_POLY. The authors thankfully acknowledge the computer resources, technical expertise, and assistance provided by the Barcelona Supercomputing Center, Centro Nacional de Supercomputación.

Supporting Information Available: Parameters describing the ions and solvent and details of the molecular dynamics simulations. This material is available free of charge via the Internet at http://pubs.acs.org.

References and Notes

(1) Wasielewski, M. R. *Chem. Rev.* **1992**, *92*, 435–446.
(2) Rowe, G. K.; Creager, S. E. *Langmuir* **1991**, *7*, 2307–2312.
(3) Barbara, P. F.; Meyer, T. J.; Ratner, M. A. *J. Phys. Chem.* **1996**, *100*, 13148–13168.
(4) Szwarc, M. *Ions and Ion Pairs in Organic Reactions*; Wiley-Interscience: New York, 1972; Vol. 1.
(5) Fu, D. X.; Libson, A.; Miercke, L. J. W.; Weitzman, C.; Nollert, P.; Krucinski, J.; Stroud, R. M. *Science* **2000**, *290*, 481–486.
(6) Thomas, A. S.; Elcock, A. H. *J. Am. Chem. Soc.* **2004**, *126*, 2208–2214.
(7) Marcus, Y.; Hefter, G. *Chem. Rev.* **2006**, *106*, 4585–4621.
(8) Chen, E. Y. X.; Marks, T. J. *Chem. Rev.* **2000**, *100*, 1391–1434.
(9) Macchioni, A. *Chem. Rev.* **2005**, *105*, 2039–2073.
(10) Bjerrum, N. *Mat.−Fys. Medd.−K. Dan. Vidensk. Selsk.* **1926**, *7*, 9.
(11) Fuoss, R. M. *J. Am. Chem. Soc.* **1958**, *80*, 5059–5061.
(12) Borel, A.; Helm, L.; Merbach, A. E. *Chem.−Eur. J.* **2001**, *7*, 600–610.
(13) Chialvo, A. A.; Cummings, P. T.; Simonson, J. M. *J. Mol. Liq.* **2003**, *103−104*, 235–248.
(14) Hawlicka, E.; Swiatla-Wojcik, D. *J. Chem. Phys.* **2003**, *119*, 2206–2213.
(15) Naidoo, K. J.; Lopis, A. S.; Westra, A. N.; Robinson, D. J.; Koch, K. R. *J. Am. Chem. Soc.* **2003**, *125*, 13330–13331.
(16) Mason, P. E.; Neilson, G. W.; Enderby, J. E.; Saboungi, M. L.; Dempsey, C. E.; MacKerell, J. A. D.; Brady, J. W. *J. Am. Chem. Soc.* **2004**, *126*, 11462–11470.
(17) Correa, A.; Cavallo, L. *J. Am. Chem. Soc.* **2006**, *128*, 10952–10959.
(18) Megyes, T.; Baků, I.; Bğlint, S.; Grůsz, T.; Radnai, T. *J. Mol. Liq.* **2006**, *129*, 63–74.
(19) Thomas, A. S.; Elcock, A. H. *J. Am. Chem. Soc.* **2006**, *128*, 7796–7806.
(20) Hill, C. L. *Chem. Rev.* **1998**, *98*, 1–2.
(21) Hill, C. L. In *Comprehensive Coordination Chemistry II: From Biology to Nanotechnology*; McCleverty, J. A., Meyer, T. J., Eds.; Elsevier Ltd.: Oxford, U.K., 2004; Vol. 4, Chapter 11, pp 679−759.
(22) Pope, M. T. In *Comprehensive Coordination Chemistry II: From Biology to Nanotechnology*; McCleverty, J. A., Meyer, T. J. , Eds.; Elsevier Ltd.: Oxford, U.K., 2004; Vol. 4, Chapter 10, pp 635−678.
(23) Muller, A.; Beckmann, E.; Bogge, H.; Schmidtmann, M.; Dress, A. *Angew. Chem., Int. Ed.* **2002**, *41*, 1162–1167.
(24) Pope, M. T.; Muller, A. *Angew. Chem., Int. Ed.* **1991**, *30*, 34–48.
(25) Hill, C. L.; Bouchard, D. A. *J. Am. Chem. Soc.* **1985**, *107*, 5148–5157.
(26) Hill, C. L.; Prossermccartha, C. M. *Coord. Chem. Rev.* **1995**, *143*, 407–455.
(27) Neumann, R.; Khenkin, A. M.; Dahan, M. *Angew. Chem., Int. Ed.* **1995**, *34*, 1587–1589.
(28) Neumann, R. *Prog. Inorg. Chem.* **1998**, *47*, 317–370.
(29) Neumann, R.; Dahan, M. *J. Am. Chem. Soc.* **1998**, *120*, 11969–11976.
(30) Rodriguez-Rivera, G. J.; Kim, W. B.; Evans, S. T.; Voitl, T.; Dumesic, J. A. *J. Am. Chem. Soc.* **2005**, *127*, 10790–10791.
(31) Muller, A.; Peters, F.; Pope, M. T.; Gatteschi, D. *Chem. Rev.* **1998**, *98*, 239–271.
(32) Burns, P. C.; Kubatko, K. A.; Sigmon, G.; Fryer, B. J.; Gagnon, J. E.; Antonio, M. R.; Soderholm, L. *Angew. Chem., Int. Ed.* **2005**, *44*, 2135–2139.
(33) Rhule, J. T.; Hill, C. L.; Judd, D. A. *Chem. Rev.* **1998**, *98*, 327–357.
(34) Zhao, F.; Gu, N.; Liu, S.; Wang, Z.; Dong, S. *Electroanalysis* **2003**, *15*, 695–701.
(35) Kim, W. B.; Voitl, T.; Rodriguez-Rivera, G. J.; Dumesic, J. A. *Science* **2004**, *305*, 1280–1283.
(36) Kim, W. B.; Voitl, T.; Rodriguez-Rivera, G. J.; Evans, S. T.; Dumesic, J. A. *Angew. Chem., Int. Ed.* **2005**, *44*, 778–782.
(37) Long, D.-L.; Cronin, L. *Chem.−Eur. J.* **2006**, *12*, 3698–3706.
(38) Muller, A.; Rehder, D.; Haupt, E. T. K.; Merca, A.; Bogge, H.; Schmidtmann, M.; Heinze-Bruckner, G. *Angew. Chem., Int. Ed.* **2004**, *43*, 4466–4470.
(39) Muller, A.; Toma, L.; Bogge, H.; Schaffer, C.; Stammler, A. *Angew. Chem., Int. Ed.* **2005**, *44*, 7757–7761.
(40) Muller, A.; Zhou, Y. S.; Bogge, H.; Schmidtmann, M.; Mitra, T.; Haupt, E. T. K.; Berkle, A. *Angew. Chem., Int. Ed.* **2006**, *45*, 460–465.
(41) Cronin, L. *Angew. Chem., Int. Ed.* **2006**, *45*, 3576–3578.
(42) Maestre, J. M.; Lopez, X.; Bo, C.; Poblet, J. M.; Casan-Pastor, N. *J. Am. Chem. Soc.* **2001**, *123*, 3749–3758.
(43) Lopez, X.; Maestre, J. M.; Bo, C.; Poblet, J. M. *J. Am. Chem. Soc.* **2001**, *123*, 9571–9576.
(44) Lopez, X.; Bo, C.; Poblet, J. M. *J. Am. Chem. Soc.* **2002**, *124*, 12574–12582.
(45) Poblet, J. M.; Lopez, X.; Bo, C. *Chem. Soc. Rev.* **2003**, *32*, 297–308.
(46) Lopez, X.; Fernandez, J. A.; Romo, S.; Paul, J. F.; Kazansky, L.; Poblet, J. M. *J. Comput. Chem.* **2004**, *25*, 1542–1549.
(47) Lopez, X.; de Graaf, C.; Maestre, J. M.; Beard, M.; Rohmer, M. M.; Bo, C.; Poblet, J. M. *J. Chem. Theory Comput.* **2005**, *1*, 856–861.
(48) Rodriguez-Fortea, A.; de Graaf, C.; Poblet, J. M. *Chem. Phys. Lett.* **2006**, *428*, 88–92.
(49) Lopez, X.; Nieto-Draghi, C.; Bo, C.; Avalos, J. B.; Poblet, J. M. *J. Phys. Chem. A* **2005**, *109*, 1216–1222.
(50) Pope, M. T.; Varga, G. M. *Inorg. Chem.* **1966**, *5*, 1249–1254.
(51) Grigoriev, V. A.; Hill, C. L.; Weinstock, I. A. *J. Am. Chem. Soc.* **2000**, *122*, 3544–3545.
(52) Grigoriev, V. A.; Cheng, D.; Hill, C. L.; Weinstock, I. A. *J. Am. Chem. Soc.* **2001**, *123*, 5292–5307.
(53) Broadwater, T. L.; Kay, R. L. *J. Phys. Chem.* **1970**, *74*, 3802–3812.
(54) Geletii, Y. V.; Hill, C. L.; Bailey, A. J.; Hardcastle, K. I.; Atalla, R. H.; Weinstock, I. A. *Inorg. Chem.* **2005**, *44*, 8955–8966.
(55) Czap, A.; Neuman, N.; Swaddle, T. *Inorg. Chem.* **2006**, *45*, 9518–9530.
(56) Ebeling, W.; Hilbert, S.; Krienke, H. *J. Mol. Liq.* **2002**, *96−97*, 409–423.
(57) Faraudo, J.; Bresme, F. *Phys. Rev. Lett.* **2004**, *92*, 236102.
(58) Ciccotti, G.; Ferrario, M.; Haynes, J. T.; Kapral, R. *Chem. Phys.* **1989**, *129*, 241–251.
(59) Qin, Y.; Prausnitz, J. M. *J. Chem. Phys.* **2004**, *121*, 3181–3183.
(60) Ebeling W.; Justice J.-C. Lars Onsager's contribution to electrolyte theory. In *The collected works of Lars Onsager (with commentary)*; World Scientific: Singapore, 1996.
(61) Fisher, M. E.; Zuckerman, D. M. *J. Chem. Phys.* **1998**, *109*, 7961–7981.
(62) Chandler, D. *Introduction to modern statistical mechanics*; Oxford University Press: Oxford, U.K.,1987.
(63) Justice, M. C.; Justice, J.-C. *J. Solution Chem.* **1977**, *6*, 819.
(64) Forester, T. R.; Smith, W.; Todorov, I. T. *The DL_POLY molecular simulation package*, version 2.15; CCLRC Daresbury Laboratory, CSE Department: Cheshire, England; http://www.ccp5.ac.uk/DL_POLY, accessed Dec 2006.
(65) Berendsen, H. J. C.; Grigera, J. R.; Straatsma, T. P. *J. Phys. Chem.* **1987**, *91*, 6269–6271.
(66) Lee, S. H.; Rasaiah, J. C. *J. Phys. Chem.* **1996**, *100*, 1420–1425.
(67) Nama, D.; Anil Kumar, P. G.; Pregosin, P. S. *Magn. Reson. Chem.* **2005**, *45*, 246–250.
(68) Kim, S.; Karilla, S. *Microhydrodynamics: Principles and Selected Applications*; Butterworth-Heinemann: Boston, 1991.
(69) Mac Quarrie, A. D. *Statistical Mechanics*; Harper Collins Publishers: New York, 1976.

JP077098P